Proceedings of CONF-MPCS 2026 Symposium: Theoretic Physics and Plasma Physics
DOI: 10.54254/2753-8818/2026.DL33421

A Study on Shanghai's Shared Bicycle Deployment Mechanism from a Human-Environment Synergy Perspective

Wenxuan An

NUIST Reading Academy, Nanjing University of Information Science & Technology, Nanjing, China
202383100036@nuist.edu.cn

Abstract. To explore the synergistic influence of built environment and user behavior on shared bicycle deployment volume, this study uses 2016 Mobike riding trajectory data from Shanghai. Integrating multi-source Point of Interest (POI), a "human-land" collaborative analysis framework is established. Spatially, Principal Component Analysis (PCA) extracts three core spatial factors—"commercial consumption," "transportation accessibility," and "residential density"—from 12 POI indicators to describe urban functional differentiation. User-wise, K-means clustering identifies three typical user groups based on riding duration, frequency, and time slots: high-frequency commuters, leisure-long-distance riders, and occasional low-frequency users. Multivariate regression examines the main and interaction effects of these spatial factors and user types on deployment volume. Results show all three spatial factors and the proportions of high-frequency commuters and leisure-long-distance users positively affect deployment volume. Interaction effects include positive synergy between "commercial consumption and high-frequency commuting," additional demand from "transportation convenience and leisure-long-distance," and tidal suppression from "residential density and high-frequency commuting." Three typical deployment paradigms (business consumption, transportation hub, high residential density) are summarized, and a meticulous, differentiated deployment strategy is proposed based on spatial zones, time periods, and user groups. These conclusions provide a solid foundation for dynamic balanced scheduling of shared bicycles and rational optimization of urban slow traffic systems.

Keywords: shared bicycles, person-place coordination, principal component analysis, K-means clustering

1. Introduction

In recent years, bike-sharing has become an integral part of urban transportation systems in China. With its rapid development, though, obvious spatiotemporal imbalances between supply and demand have emerged—specifically, "bikes are hard to find" in peak-hour commuting hotspots, while "bike congestion" plagues residential areas [1,2]. This spatiotemporal mismatch raises corporate operation costs and reduces the efficiency of urban travel. It also reflects the complex interactions inherent in typical human-environment systems: users' micro-level travel decisions and the built urban environment have a dynamic coupling mechanism, and the essence of this imbalance is the optimal

© 2026 The Authors. This is an open access article distributed under the terms of the Creative Commons Attribution License 4.0 (https://creativecommons.org/licenses/by/4.0/).

DOI: 10.54254/2753-8818/2026.DL33421

allocation of resources under the interplay of multiple factors [3,4]. This study plans to construct an optimization model based on multi-source data fusion, to clarify the spatiotemporal matching patterns of urban non-motorized transportation resources from a systems science perspective. In this way, it can provide quantitative decision support and theoretical foundations for reducing societal operational costs and enhancing travel efficiency.

On the spatiotemporal patterns of shared bicycle deployment, there have been many systematic studies from different dimensions in existing literature. In terms of environmental impact, the density, diversity, and design evaluation model put forward by Cervero and Kockelman [4] in 2003 provided a theoretical basis for analyzing cycling environments. In 2018, Wu and Ye [5] used big data to conduct in-depth spatiotemporal analysis of parking behaviors, and found that Point of Interest (POI) distribution has a significant guiding effect on bicycle parking density. Recently, in 2022, Liu et al. [6] pointed out that the environmental benefits of bicycle systems rely heavily on spatiotemporal accessibility. Dong and Liu [7] did an empirical analysis in Shanghai, exploring the complex impacts of different built environment factors on the integration of shared bicycles and rail transit. In terms of resource allocation and scheduling optimization, Fishman [1] stressed the importance of station turnover efficiency in 2016. Zhang and Zeng [8] applied machine learning algorithms to flow modeling in 2020. In 2023, Lee et al. [9] went a step further, using dynamic time warping to identify the popularity evolution patterns of different urban areas. Besides, Eren and Uz [10] systematically classified shared bicycle demand in 2020, pointing out that users' socioeconomic attributes are crucial for demand forecasting. This supplements the differences in commuters' spatial choices explored by Wang and Wang [11] in 2021. In 2025, Cai et al. [12] found that there are obvious age-related differences in people's cycling preferences for commercial and green spaces. But prior studies usually separate user behavioral characteristics from spatial and geographical attributes. They lack systematic analysis of the relationship between the two in a unified framework. Moreover, there is still a lack of in-depth research on the deployment accuracy in specific areas of megacities and how it matches user attributes.

To make up for these shortcomings, this paper takes Shanghai as a case study and builds a multidimensional analytical framework that combines user profiles and spatial attributes. From the angle of "human-environment" synergy, this study tries to find out the interactive mechanisms of how users with different attributes affect the deployment of shared bicycles in specific spatial contexts, focusing especially on identifying the core factors that shape the dominant locational functions. Different from previous studies, the innovation of this paper is that it explores the nonlinear coupling patterns between user profiles and geographic locations. By figuring out the complex mechanisms behind the spatiotemporal allocation of shared bicycles from a systemic perspective, it provides a quantitative theoretical basis for optimizing dynamic dispatch strategies and improving resource matching efficiency.

2. Materials and methods

2.1. Materials

2.1.1. Study area selection and data sources

Shanghai's central urban districts were chosen to serve as the case study area, primarily because they take a pioneering position in shared bicycle management, feature complex land use and sound transport connectivity, and boast diverse user groups shaped by a large commuter population.

DOI: 10.54254/2753-8818/2026.DL33421

The dataset comprises two major components: Shanghai shared bicycle ride data and spatial geographic information data. The shared bicycle ride data was collected from Mobike's open trajectory dataset for August 2016 in Shanghai (https://www.heywhale.com/mw/dataset/5eb6787e366f4d002d77c331/content), encompassing around 100,000 ride orders within central urban districts. Features of order ID, user ID, vehicle ID, start time, start latitude/longitude coordinates, and ride trajectory points were also included.

For the geographic data, POI for Shanghai during 2016 was scraped via the AutoNavi Maps API, which covers 12 core categories, including dining, offices, transportation facilities, residential areas, and commercial districts, used to construct the built environment indicator system. The road network and administrative boundary were sourced from the OpenStreetMap (OSM) vector database.

2.1.2. Data preprocessing

To make sure the analysis is reliable, the original dataset was processed and a density-based clustering algorithm was used to find users whose behavioral patterns were much different from the average. This step found 132 abnormal users—their average ride time was 124 minutes, which is way longer than ordinary users, and their usage time distribution was also irregular. These usage patterns might be due to data errors, food delivery riders, or other unusual ways of using shared bikes. After removing these abnormal users, 16,756 valid ones were retained, and the abnormal cases made up less than 1% of the total sample.

A spatial gridding method was then adopted, dividing the research area into 500m×500m grids as the basic analysis unit. Spatial join techniques were also used to gather the starting and ending points of trips into these grids for further analysis.

2.2. Methods

2.2.1. Principal component analysis

Principal Component Analysis (PCA) employs orthogonal transformation to convert potentially correlated variables into a set of linearly uncorrelated composite variables, known as principal components [13]. Let $\mathrm{X_i}=(\mathrm{X_{i1}},\mathrm{X_{i2}},\ldots,\mathrm{X_{ip}})^{\top}, i=1,\ldots,N$,denote the p -dimensional observed vector of built environmental indicator for the i -th grid (500m×500m). To eliminate scaling effects, each indicator is standardized via z-score transformation, resulting in zero mean and unit variance. The standardized vector is denoted as $\mathrm{Z_i}$, and the standardized data matrix for all grids is Z of dimension $\mathrm{N}\times\mathrm{p}$. The covariance matrix (i.e., correlation matrix) of the standardized data is computed as:

$$\mathrm{R}=\frac{1}{N-1}\mathrm{Z}^{\top}\mathrm{Z}. \tag{1}$$

Through spectral decomposition of covariance matrix (i.e., correlation matrix),

$$\mathrm{R}=\frac{1}{N-1}\mathrm{Z}^{\top}\mathrm{Z}=\sum_{l=1}^{p}\lambda_l \mathrm{v}_l \mathrm{v}_l^{\top}, \tag{2}$$

where $\lambda_1\geq\lambda_2\geq\ldots\geq\lambda_\mathrm{p}\geq 0$ are eigenvalues, and $\mathrm{v_l}$ are the corresponding $\mathrm{p}\times 1$ orthonormal eigenvectors (i.e., loadings). The loadings $\mathrm{v_l}$ describe the direction and contribution of original

DOI: 10.54254/2753-8818/2026.DL33421

variables to the l-th principal component (PC_l). The l-th PC values are linear combinations of the standardized variables and the loadings. For the i-th grid, the score is:

$$PC_{il} = Z_i^{\top} v_l = v_l Z_{i1} + v_l Z_{i2} + \cdots + v_l Z_{ip}, \tag{3}$$

where the vector PC_l of values across all grids has mean zero and variance λ_l , and distinct PCs are uncorrelated. The variance explained by PC_l is $\lambda_l / \sum_{j=1}^{p} \lambda_j$, and the cumulative variance explained by the first m components is $\sum_{l=1}^{m} \lambda_l / \sum_{j=1}^{p} \lambda_j$ .PCs are retained based on the eigenvalue-greater-than-one criterion, requiring the cumulative explained variance to exceed 70% to ensure that the extracted components adequately capture the main information structure of the original variables.

Before extracting the principal components, the data's suitability for aggregation was evaluated via the Kaiser-Meyer-Olkin (KMO) test and Bartlett's test of sphericity [14,15]. A KMO value above 0.7 indicates strong common variance, while a significant Bartlett's test ($p<0.05$) confirms that the variables are sufficiently correlated. In this study, the KMO value of 0.826 and a highly significant Bartlett's result ($p<0.001$) indicate that the dataset is well-suited for PCA.

To enhance interpretability, the loading matrix was orthogonally rotated using the Varimax method [16]. This rotation ensures that each component exhibits distinct semantic meaning based on high-loading variables, allowing the resulting factors to be clearly defined as core indicators of urban spatial functional differentiation.

2.2.2. Cluster analysis

K-Means clustering is a prototype-based partitioning algorithm that partitions N samples into K disjoint clusters, minimizing intra-cluster variance. Given M users, each characterized by q behavioral features, let $w_i = (w_{i1}, \ldots, w_{iq})^{\top} \in R^q$ denote the feature vector of the i-th user, and $W = (w_1, \ldots, w_M)^{\top} \in R^{M \times q}$ the data matrix. The algorithm partitions users into clusters $C_1, \ldots, C_K$ with centroids $\mu_j = \frac{1}{|C_j|} \sum_{w_i \in C_j} w_i$. The objective function is:

$$J = \sum_{j=1}^{K} \sum_{w_i \in C_j} \| w_i - \mu_j \|^2. \tag{4}$$

To characterize user behavior, seven features are extracted: total orders, average trip duration, weekday usage ratio, morning peak ratio, evening peak ratio, peak concentration (P), and temporal entropy(H). Peak concentration measures the proportion of trips during morning and evening peaks:

$$P = \frac{N_{peak_morning} + N_{peak_evening}}{N_{total}} \tag{5}$$

Here, $N_{peak_morning}$ and $N_{peak_evening}$ represent the number of orders placed by users during the morning and evening rush hours, respectively, while N_{total} represents the total number of orders placed by users. Temporal entropy quantifies the dispersion of trip times using Shannon entropy $H = -\sum_{i=1}^{24} p_i \log(p_i)$,where a 24-hour day is divided into n time slots (with each slot being one hour, where n = 24), and p_i represents the proportion of the user's orders in the i-th time slot relative to the total number of orders.

DOI: 10.54254/2753-8818/2026.DL33421

2.2.3. Multiple linear regression

Multiple linear regression quantifies the linear relationship between a continuous dependent variable and multiple independent variables. This study applies it to examine the main and interaction effects of spatial factors and user types on bike-sharing deployment. Let there be N grids of 500m×500m each serving as an independent observation. For grid m, the dependent variable Y_m is the bike deployment volume, approximated by the total number of trip origins and destinations within the grid.

For explanatory variables, first, spatial factor values $PC_{1m},\ldots,PC_{am}$, where a is the number of factors extracted via PCA. Second, user type proportions $R_{1m},\ldots,R_{bm}$, where b is the number of user types identified via K-Means clustering. Third, interaction terms between spatial factors and user proportions to capture synergistic or inhibitory effects. The general regression model is then:

$$Y_m=\beta_0+\sum_{i=1}^{a}\beta_i PC_{im}+\sum_{j=1}^{b}\gamma_j R_{jm}+\sum_{i=1}^{a}\sum_{j=1}^{b}\delta_{ij}(PC_{im}\times R_{jm})+\varepsilon_m, \tag{6}$$

where β_0 is the intercept, β_i and γ_j are main effect coefficients, δ_{ij} are interaction coefficients, and ε_m is the error term assumed to follow $N(0,\sigma^2)$. The model is estimated via ordinary least squares (OLS), which minimizes the sum of squared residuals:

$$\min_{\beta,\gamma,\delta}\sum_{m=1}^{M}(Y_m-\hat{Y}_m)^2, \tag{7}$$

where $\hat{Y}_m$ denotes the fitted value. Model fitness is assessed using two metrics. The coefficient of determination R^2 given by

$$R^2=1-\frac{\sum_{m=1}^{M}(Y_m-\hat{Y}_m)^2}{\sum_{m=1}^{M}(Y_m-\bar{Y})^2} \tag{8}$$

where $\bar{Y}$ is the sample mean of the dependent variable. R^2 ranges from 0 to 1, with higher values indicating better fit.

All continuous predictors are standardized to zero mean and unit variance before estimation to ensure coefficient comparability. The analyses were conducted using SPSS for principal component analysis and Python for clustering and regression modeling.

3. Results

3.1. PCA in spatial dimensions

Applying the PCA, the eigenvalues and contribution proportions for the 12 PCs were shown in Table 1. Following the principle of selecting components with eigenvalues greater than 1, the study selected the top three PCs for in-depth analysis. The cumulative variance explained by PC1, PC2, and PC3 reached 74.702%, indicating that these three composite factors can represent the vast majority of the information content of the original environment indicators.

DOI: 10.54254/2753-8818/2026.DL33421

Table 1. Result of variance explained in PCA

Component No.	Initial Eigenvalue	Variance Contribution (%)	Cumulative Variance Contribution (%)
PC1	4.821	43.807	43.807
PC2	2.152	19.554	63.361
PC3	1.248	11.341	74.702
PC4	0.854	7.759	82.461
PC5	0.532	4.834	87.295
PC6	0.411	3.735	91.030
PC7	0.325	2.953	93.983
PC8	0.241	2.189	96.172
PC9	0.187	1.699	97.871
PC10	0.112	1.018	98.889
PC11	0.081	0.736	99.625
PC12	0.041	0.375	100.000

To enhance interpretability, the original factor loading matrix was rotated using the maximum variance method, with the rotated loading matrix shown in Table 2. Analysis reveals that Shanghai's central urban area spatial environment characteristics can be summarized into three core factors: The PC1 exhibits loadings exceeding 0.7 across indicators such as office buildings, financial institutions, and dining establishments, reflecting the area's commercial office and consumer vitality. It is named the "Commercial Consumption Factor". The PC2 exhibits prominent loadings on subway station density, bus stop density, and road network density, reflecting the connectivity efficiency of transportation hubs. It is named the "Transportation Accessibility Factor." The PC3 shows high positive loadings on residential complex entrances/exits and population density indicators, representing fundamental residential attributes. It is named the "Residential Intensity Factor."

Table 2. Rotated factor loadings matrix

Original Indicator Variables	Business Consumption Factor (PC1)	Transportation Accessibility Factor (PC2)	Residential Intensity Factor (PC3)
Number of Office Buildings	0.852	0.124	0.056
Number of Food and Beverage Establishments	0.814	0.210	0.112
Number of shopping centers	0.789	0.156	0.043
Subway station density	0.105	0.887	0.094
Bus stop density	0.211	0.765	0.158
Road network density	0.324	0.712	0.088
Residential Area Entrances/Exits	0.082	0.045	0.912
Population Density Estimate	0.156	0.234	0.845

3.2. Cluster analysis from the user perspective

Based on the principles of the clustering analysis and the seven features' metrics identified, the results show that dividing users into three clusters yields optimal intra-cluster cohesion and inter-

DOI: 10.54254/2753-8818/2026.DL33421

cluster separation. Therefore, the 16,756 users were classified into three representative groups, named R1, R2 and R3. Based on four dimensions—number of orders, ride duration, proportion of rides on weekdays, and departure time—this paper profiles and analyses the behavior of each user group (Table 3 and Figure 1). The first group, high-frequency commuters (R1), shows high order volume, a large share of weekday rides, high route repetition, relatively short average ride duration, and travel times heavily focused on morning and evening rush hours. Their spatial distribution features typical "residential area–business district" point-to-point movement, reflecting strong commuting attributes. The second group, Leisure/Long-distance users (R2), has more dispersed riding trajectories, longer average ride durations, and travel times mainly concentrated around noon and evening. Their spatial distribution clusters in commercial districts, tourist attractions, and green spaces, reflecting non-essential travel driven by leisure and entertainment. The third group, occasional users (R3), is a smaller overall group with fewer orders, shorter ride durations, and a low share of weekday trips. Their travel times have no clear pattern, with the coefficient of variation exceeding 45% across all behavioral metrics, classifying them as a low-frequency, random-use group.

Table 3. User profile table

User Type	Number of Orders	Ride Duration	Departure Time	Weekday Ratio	Behavioral Characteristics Summary
High-frequency Commuters (R1)	High	Low-to-Moderate	Morning Rush Hour	High (>80%)	Distinct commuting behavior, stable frequency
Leisure/Long-distance users (R2)	Medium	High	Midday/Evening	Moderate (approx. 50%)	Weekend trips or non-essential travel
Occasional users (R3)	Low	Low	Time dispersion	Low (<50%)	Low usage frequency, highly irregular

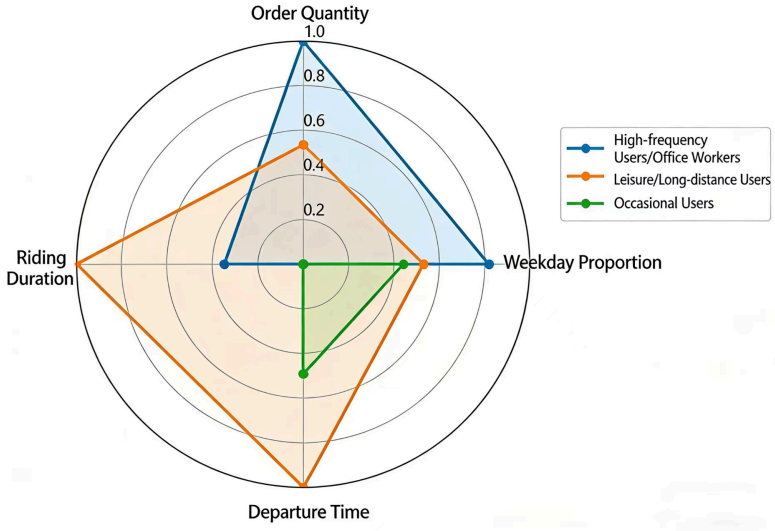


Figure 1. User type profile radar chart

DOI: 10.54254/2753-8818/2026.DL33421

3.3. Comprehensive analysis of deployment mechanisms

In the regression model, the independent variables were organized based on the PCs and clusters: the three spatial factors (Business Consumption Factor PC1, Transportation Convenience Factor PC2, and Residential Density Factor PC3); the proportion of orders from the three user categories (High-Frequency Commuters R1, Leisure Long-Distance Travelers R2, Occasional Low-Frequency Type R3), as well as all interaction terms among these six variables ($PC_i \times R_j; i = 1,2,3; j = 1,2,3$). The regression results are shown in Table 4.

Table 4. Regression model results for influencing factors

Variable	Coefficient	Standard Error	t-value	p-value
Constant	124.53	8.76	14.22	<0.001
Business Consumption Factor (PC_1)	36.21	3.45	10.50	<0.001
Transportation Convenience Factor (PC_2)	28.74	3.12	9.21	<0.001
Residential Density Factor (PC_3)	15.33	2.98	5.14	<0.001
High-frequency commuter share (R_1)	42.67	5.21	8.19	<0.001
Leisure long-distance commuters (R_2)	18.92	4.76	3.98	<0.001
Occasional low-frequency type proportion (R_3)	2.34	2.01	1.16	0.245
$PC_1 \times R_1$	21.35	3.89	5.49	0.000
$PC_1 \times R_2$	4.28	3.57	1.20	0.231
$PC_1 \times R_3$	-1.96	3.12	-0.63	0.529
$PC_2 \times R_1$	3.28	2.76	1.19	0.234
$PC_2 \times R_2$	9.86	4.12	2.39	0.017
$PC_2 \times R_3$	2.15	2.89	0.74	0.458
$PC_3 \times R_1$	-12.43	3.67	-3.39	0.001
$PC_3 \times R_2$	3.67	3.21	1.14	0.254
$PC_3 \times R_3$	1.82	2.54	0.72	0.472

DOI: 10.54254/2753-8818/2026.DL33421

Table 4. (continued)

R^2	0.742	—	—	—

Based on the regression results, the R^2 of the model is 0.742, indicating that the model has good explanatory power. Regarding main effects, all three spatial factors exerted significant positive impacts on deployment volume, with the commercial consumption factor contributing most substantially (coefficient 36.21), indicating the strongest demand for shared bikes in densely commercialized office districts. Among user types, the high-frequency commuter segment yielded the highest coefficient (42.67), followed by the leisure/long-distance segment (18.92). The occasional/low-frequency segment showed an insignificant coefficient, suggesting its highly random behavior provides no stable contribution to deployment volume.

Interaction term analysis revealed the underlying mechanisms of "person-place" synergy. The coefficient of $PC_1 \times R_1$ was significantly positive (21.35), indicating that in areas with high commercial consumption factors, an increase in the proportion of high-frequency commuters further amplifies deployment demand—demonstrating a synergistic enhancement effect between the business environment and commuter users. The coefficient of $PC_2 \times R_2$ is significantly positive (9.86), indicating that an increase in leisure users in areas with convenient transportation also generates additional deployment demand. The coefficient of $PC_3 \times R_1$ is significantly negative (-12.43), meaning that in areas with high residential density, an increase in the proportion of high-frequency commuters actually reduces the growth rate of deployment volume.

The deployment mechanism of shared bicycles in Shanghai's central urban area can be categorized into three typical patterns. Commercial-oriented areas are dominated by the commercial consumption factor, with high-frequency commuters as the primary user group, exhibiting a tidal demand pattern concentrated during morning and evening peak hours. Transportation hub areas are dominated by the transportation accessibility factor, with both high-frequency commuters and leisure long-distance users as the main user groups, generating all-day transfer demand with further concentration during peak hours. Residential-dense areas are dominated by the residential density factor, with high-frequency commuters as the primary user group, characterized by a tidal suppression effect where a large number of bicycles depart during morning peak and return in concentrated fashion during evening peak.

4. Discussion

This study constructs a "human-environment synergy" framework to explore the interactive mechanisms of spatial factors and user types on the deployment volume of shared bicycles in central Shanghai. The results show three spatial factors—commercial consumption, transportation accessibility, and residential density—and two user groups—high-frequency commuters and leisure long-distance users—as significant positive influencing factors. Interaction effects also reveal three underlying mechanisms: synergistic enhancement between commercial consumption and commuters, demand pull between transportation accessibility and leisure users, and tidal suppression between residential density and commuters.

Based on these findings, three distinct deployment patterns stand out. Commercial-oriented areas, mainly shaped by commercial consumption and high-frequency commuters, show a tidal demand pattern that's focused on peak hours. This is driven by the synergistic reinforcement between the commercial environment and commuting behavior. Transportation hub areas, affected by high

DOI: 10.54254/2753-8818/2026.DL33421

accessibility and a mix of commuters and leisure users, have sustained transfer demand throughout the day with peak-hour surges. This comes from the superposition of stable commuting needs and the extra demand pulled by leisure riders. Residential-dense areas, dominated by residential density and high-frequency commuters, have a tidal suppression effect—there are significant bicycle outflows during the morning peak, followed by concentrated returns in the evening. As a result, this study proposes a refined scheduling strategy divided by functional zone, time window, and user group.

These results not only match but also further develop the existing research. In terms of space, the three factors extracted through PCA are consistent with the classic "density, diversity, design" framework established by Cervero and Kockelman [4]. They also quantify the different contributions of each factor, showing that commercial consumption has the most significant impact on deployment demand. This supplements the research [5] on the connection between POI distributions and parking density, and also adds necessary detail by distinguishing how specific functional zones affect deployment volumes. From the user's perspective, the three identified user types are consistent with the behavioral patterns [10-11]. But this study takes it a step further, integrating user typologies with spatial factors to find their non-additive interaction effects. Different from previous studies that usually separate spatial and user dimensions [1, 7, 9], this research clearly models their interaction, providing a more detailed understanding of the human-environment coupling inherent in bike-sharing systems.

There are several limitations that need to be noted. First off, the dataset comes from Mobike's August 2016 ride records, which is the early stage of China's bike-sharing industry—this was before there were widespread regulatory measures like geo-fencing and mandatory docking zones. Second, the data are from a single operator and lack user socioeconomic attributes, which might lead to selection bias and make it hard to fully explain behavioral heterogeneity. Third, built environment indicators only include POI categories, failing to cover micro-scale factors such as cycling infrastructure quality, street greenery, or perceived safety—and all these factors could affect ridership. Fourth, the linear regression model does well in identifying main and interaction effects, but it can't pick up potential nonlinearities.

5. Conclusion

This study sets up a "human-environment synergy" framework that combines spatial factors and user types to explore the interactive mechanisms influencing shared bicycle deployment volume in central Shanghai. Based on the study's results, three typical deployment patterns are defined, and a refined scheduling strategy—divided by zone, time, and user group—is proposed. Future research can focus on multi-operator and more recent data, expand environmental and user-side indicators, and adopt nonlinear modelling methods to further improve explanatory power and applicability.

References

[1] Fishman, E. (2016) Bikeshare: A Review of Recent Literature. Transport Reviews, 36, 92-113.
[2] Shaheen, S.A., Guzman, S. and Zhang, H. (2010) Bikesharing in Europe, the Americas, and Asia: Past, present, and future. Transportation Research Record: Journal of the Transportation Research Board, 2143, 159-167.
[3] Handy, S.L., Cao, X. and Mokhtarian, P.L. (2005) Correlation or causality between the built environment and travel behavior? Evidence from Northern California. Transportation Research Part D: Transport and Environment, 10, 427-444.
[4] Cervero, R. and Kockelman, K. (2003) Travel demand and the 3Ds: Density, diversity, and design. Transportation Research Part D: Transport and Environment, 2, 199-219.

DOI: 10.54254/2753-8818/2026.DL33421

[5] Wu, Z. and Ye, Z. (2018) Spatiotemporal Characteristics of Shared Bicycle Parking Based on Big Data Analysis. Journal of Urban Planning, 5, 88-95.
[6] Liu, Y., Tian, Z., Pan, B., Zhang, W., Liu, Y., and Tian, L. (2022) A hybrid big-data-based and tolerance-based method to estimate environmental benefits of electric bike sharing. Applied Energy, 315, 118944.
[7] Dong, H. and Liu, J. (2025) Nonlinear effects of built environment on bike-sharing rail transit transfers. Modeling and Simulation, 14, 138-150.
[8] Zhang, N. and Zeng, Z. (2020) Spatiotemporal Distribution Characteristics and Deployment Volume Prediction of Urban Shared Bicycles. Transportation Systems Engineering and Information, 20, 112-118.
[9] Lee, CKH. and Leung, EKH. (2023) Spatiotemporal analysis of bike-share demand using DTW-based clustering and predictive analytics. Transportation Research Part E: Logistics and Transportation Review, 180, 103350.
[10] Eren, E. and Uz, V.C. (2020) A review on bike-sharing systems and bike-sharing demand classification. Sustainable Cities and Society, 58, 102132.
[11] Wang, Z. and Wang, L. (2021) Empirical Analysis of Shared Bicycle Users' Riding Characteristics and Influencing Factors: A Case Study of Tianjin. Soft Science, 35, 120-126.
[12] Cai, X., Gu, X., Silm, S., Hadachi, A., Jin, T., and Witlox, F. (2025) Differences in bike-sharing usage and its associations with station-surrounding characteristics: A multi-group analysis using machine learning techniques. Journal of Transport Geography, 125, 104201.
[13] Jolliffe, I.T. (2002) Principal Component Analysis. New York: Springer.
[14] Kaiser, H.F. (1970) A second generation little jiffy. Psychometrika, 35, 401-415.
[15] Bartlett, M.S. (1950) Tests of significance in factor analysis. British Journal of Statistical Psychology, 3, 77-85.
[16] Kaiser, H.F. (1958) The varimax criterion for analytic rotation in factor analysis. Psychometrika, 23, 187-200.